Numerical study of residual stress fields after double-sided symmetric laser shock peening of blade edge

Mariia L. Bartolomei, Igor S. Kudryashev, Rustam R. Sabirov
Institute of Continuous Media Mechanics of the Ural Branch of Russian Academy of Science (ICMM UB RAS), Russia
bartolomei.m@icmm.ru, http://orcid.org/0009-0003-3193-7605
i.s.kudryashev@gmail.com
sabirov@pspu.ru, http://orcid.org/0000-0002-9773-6561

Alexander M. Korsunsky
HSM Lab, Skolkovo Institute of Science and Technology, Russia; CASM&T, Advanced School of Engineering, Moscow Aviation Institute, Russia
a.korsunsky@skoltech.ru, http://orcid.org/0000-0002-3558-5198

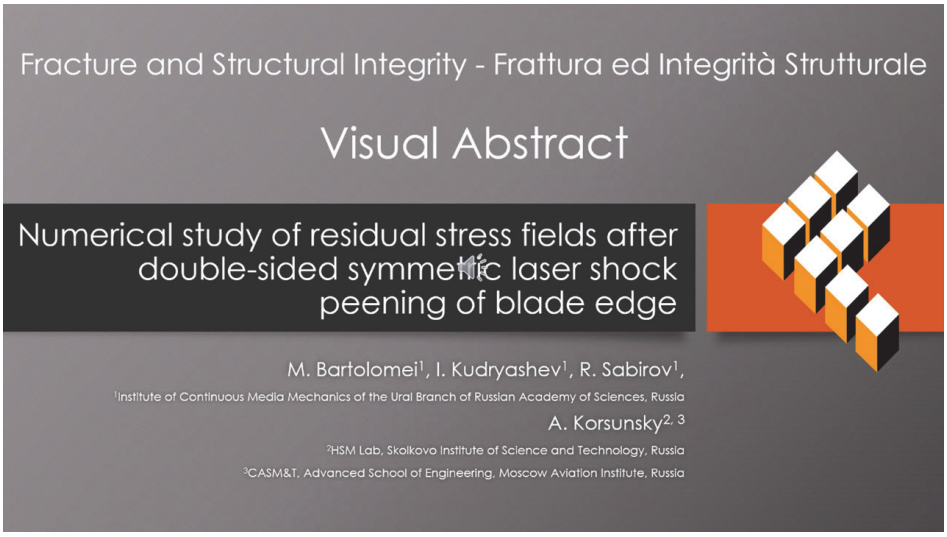

Citation: Bartolomei, M., Kudryashev, I., Sabirov, R., Korsunsky, A., Numerical investigation of residual stresses on a thin blade edge after double-sided symmetric laser shock peening, Frattura ed Integrità Strutturale, 72 (2025) 26-33.

Received: 02.12.2024
Accepted: 20.12.2024
Published: 07.01.2025
Issue: 04.2025

KEYWORDS. Laser shock peening, Numerical modeling, Titanium alloy, Residual stress.

INTRODUCTION

Increasing the fatigue life of parts and constructions remains an urgent task in aircraft industry. One of the ways to extend fatigue life is to create a near-surface layer in material with compressive residual stresses. Laser shock peening (LSP) is one of the most promising methods of residual stress creation. In order to achieve optimal distribution of residual stress, it is necessary to accurately select the parameters of the laser pulse impact. Treatment of various parts, among

which there is a large number of thin-walled parts (such as blades of aircraft turbines) is a particularly important issue, as the operating characteristics of modern equipment directly depend on it. The main type of treatment used is the method of creating residual compressive stresses in the part, which significantly increases its strength characteristics, wear resistance, corrosion resistance and durability [1-4]. Also, it allows slowing down the formation and growth of cracks [5]. A lot of ways to achieve this effect are known: mechanical shot peening, extrusion peening, rolling peening, etc. [6-8].

The LSP is a material processing method that produces compressive stresses on the surface of the material. This method allows to achieve greater depth and larger compressive stresses in contrast to the usual processing methods [7, 8]. Also, one of the advantages of the method is less damage to the samples in the process of treatment [9], which is provided due to the sectoral inline treatment, that, in turn, allows to process the complex geometry and create residual compressive stresses in the treated zone, which is most exposed to impact and prone to failure, and tensile stresses to be located in a less critical zone, in the thickened area of the base [10]. But there is a problem during LSP of thin-walled specimens as there is deformation of the geometry [11]. In this case, double-sided symmetric laser shock peening is proposed. It is assumed that with equal pressure from both sides, the deformations occurring in the workpiece will be compensated. In addition, due to the small thickness of the specimens, it is possible to create compressive stresses throughout the depth of the treated zone, which will lead to greater hardening of the material [12].

This work is devoted to numerical investigation of the effect of double-sided symmetric LSP on the generation of residual stress in a thin edge of turbine blade from TC4 titanium alloy. The process of 3D finite-element model of the LSP process in more detail is described in [13]. The calculation is carried out in two stages: first, the dynamic problem of elastic-plastic wave propagation induced by laser impact is solved; second, the static problem is solved to determine the stress field distribution. Plastic deformation after laser impacts is generated using the associated yield flow rule with the Johnson-Cook plasticity model. To verify the numerical model the residual stress profile along the depth of the specimen was compared with the data obtained by hole drilling method. The measurements were carried out for a square specimen of 2 mm thickness. And also, the profile of residual stresses after double-sided symmetric process along the depth of the thin specimen, obtained by numerical modelling results was compared with the data measured experimentally by X-ray diffraction and described in [14]. The model was used to obtain distribution of residual stresses under various double-sided symmetric peening modes. On the basis of the numerical results a database for further training of the neural network was formed.

NUMERICAL SIMULATION OF THE LASER SHOCK PEENING

The modelling of the laser shock peening treatment does not consider the process of material evaporation from the surface and the formation of high-pressure plasma. The influence of the laser pulse is taken into account by setting a time-dependent mechanical pressure function on the specimen surface. The calculation of the stress-strain state caused by this loading is performed in the finite element formulation in Ansys LS-Dyna. The problem was solved in a three-dimensional formulation taking into account the finite size of the laser spot.

In the considered problem for samples from titanium alloy TC4 the equation for calculating plastic deformations was determined by the Johnson-Cook model. Since it has a simple enough procedure for identification of material constants and it has the ability to describe the elastic-plastic wave propagation in the material with high accuracy. The LSP is examined as a mechanical process only, so the variables related to temperature effects were not taken into account [15], and the Johnson-Cook plasticity model can be written as:

$$F = \sigma_{eq} - \left[A + B\left(\varepsilon_{eq}^{pl}\right)^{n} \right] \left[1 + C \ln \frac{\dot{\varepsilon}_{eq}^{pl}}{\dot{\varepsilon}_{0}} \right] \tag{1}$$

where σ_{eq} – is the equivalent stress, ε_{eq}^{pl} – is the equivalent plastic strain, $\dot{\varepsilon}_{eq}^{pl}$ – is the equivalent plastic strain rate, $\dot{\varepsilon}_{0}$ – is a reference plastic strain rate, A, B, C, n – are parameters characterizing the inelastic behavior of the material.

For titanium alloy TC4 the following physical-mechanical constants (the elastic behavior of the alloy is described by Hooke's law for isotropic material) and Johnson-Cook model parameters were assumed in the calculation: Young's modulus E=106.7 GPa; Poisson's ratio ν=0.341; density ϱ=4424 kg/m^3; quasi-static yield stress A=978 MPa; strengthening coefficient B=826 MPa; strengthening coefficient n=0.639; strain rate sensitivity parameter C=0.034; reference plastic strain rate $\dot{\varepsilon}_0$=0.005. The determination of Johnson-Cook model parameters was performed earlier and described in [13].

An important issue for mathematical model verification process is the time duration and shape of the pressure pulse. The pressure pulse generated by laser was measured with using Photonic Doppler Velocimetry (PDV). PDV is hardware and software setup, which realize a Fourier analysis of a heterodyne laser interferometry. The basic mechanism of PDV is the investigation of interference patterns of two electromagnetic waves with a small difference in frequency. Free surface velocity of samples made from titanium alloy TC4 under the influence of laser pulse was measured using the PDV. Round specimens with a diameter of 20 mm and thickness of 0.8, 1 and 1.4 mm were used.

The shape of the laser beam profile was a circle with a diameter of 2 mm. The pulse duration was 10 ns. Measurements were performed with energies of 2, 4, 6, 8 J, which corresponded to energy power densities of 6.37, 9.55, 12.74, 19.11 GW/cm^2. The laser shot was performed into the centre of the sample and water was used as a confining layer. The results of measurements of free surface velocity profiles are presented in Figure 1 as example for circle spot with 2 mm in diameter. With a laser pulse duration of 10 ns, the duration of the pressure impulse can reach hundreds of nanoseconds and the duration would increase as it penetrates into the material due to the wave dispersion. As a hypothesis, let's approximate a pressure impulse in the form of a trapezoid. One side of the trapezoid corresponds to the plasma heating with pressure increasing. The upper base of the trapezoid corresponds to the initial expansion period with a constant pressure value. The second side of the trapezoid is the hydrodynamic expansion of the plasma with a falling pressure value.

The approximation of the time durations to zero specimen thickness gives the following values for the rise and decrease times of the pressure pulse. The rise time is 12 ns (which correlates well with the heating time), the time of constant pressure value is about 6 ns, and the pressure decrease time during the hydrodynamic expansion of the plasma is about 60 ns

The experimental value of pressure amplitude on the specimen surface was obtained through the extrapolation of the experimental results on the zero thickness specimen (Table 1). Pressure values for other power densities were approximated by data in Table 1.

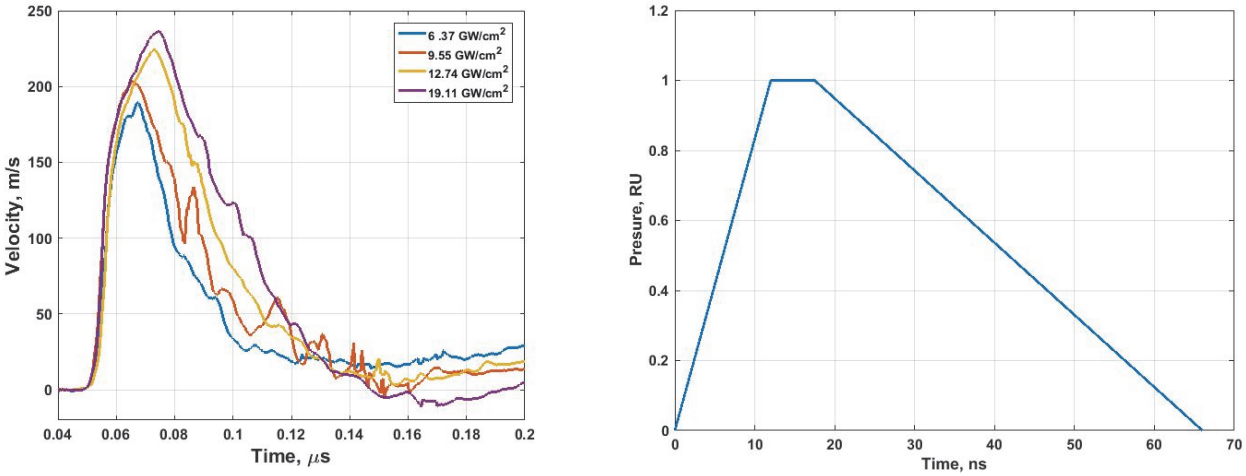

(a) (b)

Figure 1: The free surface velocity (a), the time duration and shape of the pressure pulse (b) of TC4 specimens with a thickness of 0.8 mm (averaging over 6-8 profiles).

Power density, GW/cm^2	Pressure for TC4 samples, GPa
6.37	3.00
9.55	4.00
12.74	6.00
19.11	6.50

Table 1: Experimentally measured values of pressure amplitude.

MODEL VERIFICATION

Verification of the proposed mathematical model was performed by comparing the results of calculation of the residual stresses profile measured experimentally with the data of numerical modelling for plate samples from TC4 with 2 mm thickness. Figure 2 shows the treatment scheme of the specimen (red lines show the direction of treatment) and the finite element (FE) discretization. The computational domain was discretized using 8-node hexahedral finite elements with linear shape functions. The mesh was densified near the place of load application and consisted of elements with a side size of 20 μm. As the distance to the plate boundaries increased, the side size of the element was increased to 2000 μm. The total number of elements of the computational grid was 318780.

An automatic system MTS3000-Restan (according to ASTM E837-13a [16]) was used to measure the values of residual stresses as a function of the depth of the treated layer using the hole drilling method. The averaging area for residual stress distribution in FE modelling corresponded to the drill size in the experiment and was equal to 1.6 mm in diameter. Comparison was conducted for impact of a laser beam with circle spot size 2mm in diameter, power density of 9.55 GW/cm^2 (which is equal to 4 GPa according to PDV data) with 50% overlapping.

The following boundary conditions were used in the numerical calculation: the bottom surface of the plate was fixed (no vertical displacements), the side surfaces of the plate are free of load, mechanical pressure is set in the treatment zone located on the top surface.

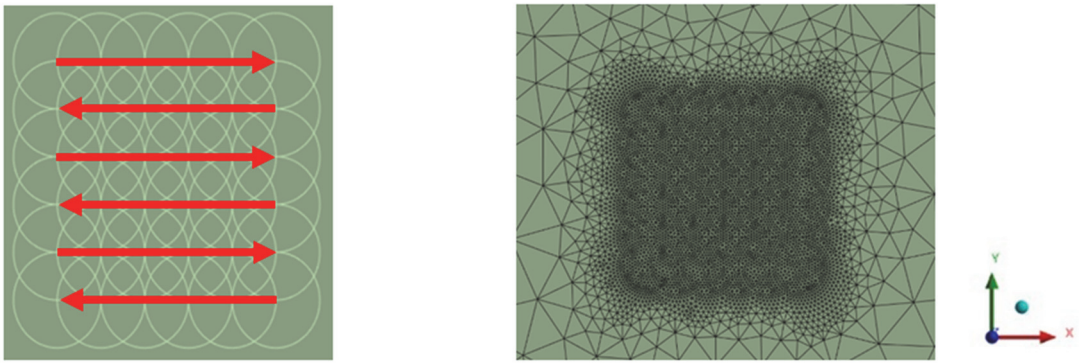

(a) (b)

Figure 2: Treatment scheme (a), the FE model (b).

An example of residual stress distribution in depth for the numerical and experimental (hole drilling) profile is shown in Figure 3 for the stress tensor component σ_x. The residual stress components σ_x and σ_y have close values at all depths, indicating the isotropy of the generated residual stresses at the surface. The principal stress σ_2 also has close values to σ_x and σ_y, so the residual stress distribution for the principal stresses σ_2 is given below. The maximum value of the compressive residual stress components is approximately 250 MPa and the depth of the formed compressive residual stress field is about 0.75 mm.

The difference in values of residual stresses in depth between experimental and numerical results is less than 10%. Thus, it can be concluded that the above numerical model well describes the distribution of residual stress fields during the processing of 2 mm thick plates. It should be noted that during LSP of thin edges the waves formed as a result of plasma expansion can lead to the formation of tensile stresses on the treated surface. In order to avoid such a negative effect, it is recommended to use double-sided symmetric LSP. Also, double-sided symmetric LSP of thin products leads to a more uniform distribution of residual stresses on the treated surface and reduces the value of product deformation [3,14,17].

To evaluate the suitability of the numerical model, the stress distribution for double-sided symmetric LSP of a thin plate is considered. The treatment scheme is similar to the one considered earlier (Fig. 2), except that the plate thickness is 0.35 mm and the impact is applied from both sides at once. During double-sided symmetric treatment the laser energy is split in half, so the pressure applied to each treated side also is reduced in half (e.g., for power density of 9.55 GW/cm^2 the pressure on each side is equal to 2 GPa). The numerical simulation data were compared with the results obtained by the authors in [14], where a specimen of the same thickness was processed, and the residual stresses were measured by X-ray diffraction. Figure 4 shows a comparison of residual stress profiles over the entire plate thickness. The results of numerical modelling of the stress distribution after double-sided symmetric LSP also correspond well to the experimental data.

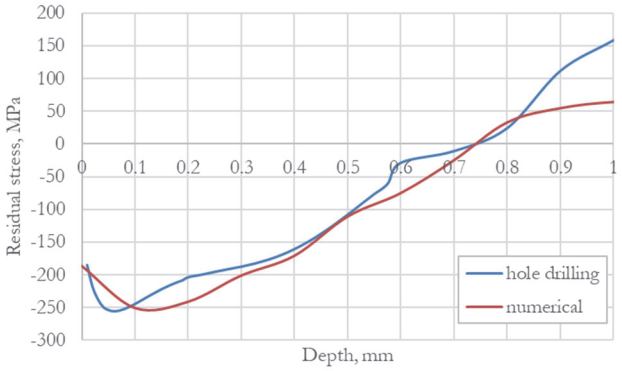

Figure 3: Residual stress in depth for 2mm plate.

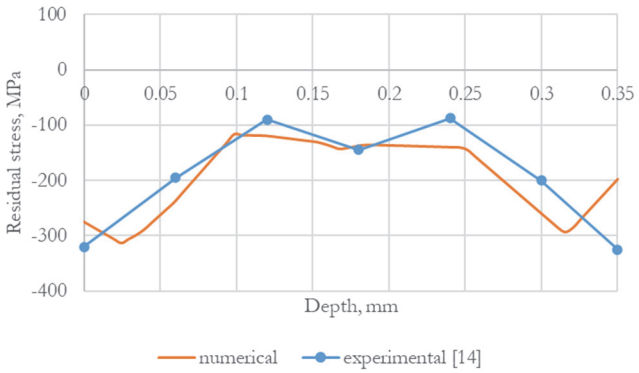

Figure 4: Residual stress in depth after double-sided symmetric LSP of 0.35 mm plate.

RESULTS AND DISCUSSION

The above explained model was applied to predict residual stress distribution induced by double-sided symmetric LSP of turbine blade edges. The purpose of numerical modelling was to determine how different processing parameters (spot shape and size, power, % overlapping, number of passes) affect the character of residual stress distribution along the blade edge thickness. And according to the results of numerical experiments to prepare a database for the beginning of artificial neural network training for calculation the optimal parameters of pulse impact during LSP. The numerical model of the blade is shown in Fig. 5. To reduce the calculation time and save computational resources, half of the blade was considered, and only the selected fragment was processed. The thickness of the blade edge in the considered section is 0.63 mm. Calculations were carried out for 34 processing variants, the parameters are given in Table 2.

The obtained residual stress distribution profiles along the thickness of the considered area are shown in Figure 6. The certain machining modes can lead to the formation of tensile residual stresses on the blade edge surface caused by the re-reflection of shock waves from each other and from free surfaces. The effective machining mode is the one that forms compressive stresses over the entire thickness of the blade edge. The presence of tensile stresses leads to a decrease in the operating characteristics of the product. For most of the calculated variants, tensile stresses are formed on the surfaces and compressive stresses are formed in the middle: these variants are not suitable for the task at hand. The situation is similar for the reverse case, where compressive stresses are at the boundaries and tensile stresses in the middle. In the case of circle spots with 30% overlapping with the minimum and maximum pressures, the stresses on the entire line under investigation lie in the negative zone (Fig. 6), which is necessary for specimen strengthening. These include: variants 7 and 9, which lie in the zone of compressive stresses, as well as 32 and 34, whose compressive stresses are minimal at the boundaries among the presented variants and are of the greatest interest in the study. For variants 7 and 9 power density is really low that it does not actually lead to the formation of residual stresses.

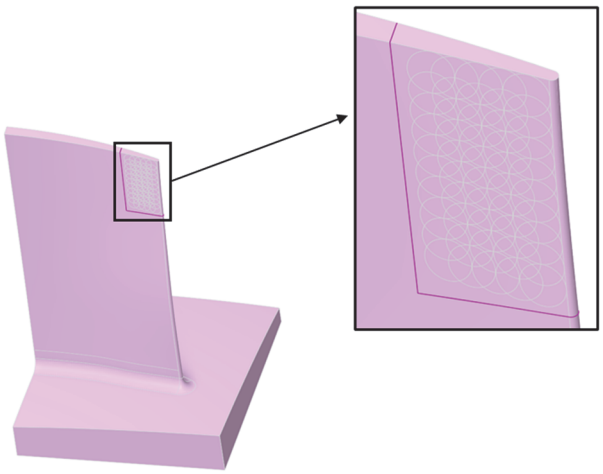

Figure 5: The blade's model and treated area.

№	Energy, J	Number of passes	Overlapping, %	Spot shape	Size, mm	Power density, GW/cm²
1	1	1	0	square	1	10
2	1	1	30	square	1	10
3	1	1	50	square	1	10
4	1	2	0	square	1	10
5	1	2	30	square	1	10
6	1	2	50	square	1	10
7	1	1	30	circle	2	3.18
8	1	1	50	circle	2	3.18
9	1	2	30	circle	2	3.18
10	1	2	50	circle	2	3.18
11	2	1	0	square	1	20
12	2	1	30	square	1	20
13	2	2	0	square	1	20
14	2	2	30	square	1	20
15	2	1	30	circle	2	6.37
16	2	1	50	circle	2	6.37
17	2	2	30	circle	2	6.37
18	2	2	50	circle	2	6.37
19	3	1	30	circle	2	9.55
20	3	1	50	circle	2	9.55
21	3	2	30	circle	2	9.55
22	3	2	50	circle	2	9.55
23	4	1	30	circle	2	12.74
24	4	1	50	circle	2	12.74
25	4	2	50	circle	2	12.74
26	5	1	30	circle	2	15.92
27	5	2	30	circle	2	15.92
28	6	1	30	circle	2	18.84
29	6	2	30	circle	2	18.84
30	6	1	50	circle	2	18.84
31	7	1	30	circle	2	21.98
32	7	2	30	circle	2	21.98
33	8	1	30	circle	2	25.48
34	8	2	30	circle	2	25.48

Table 2: Processing variants.

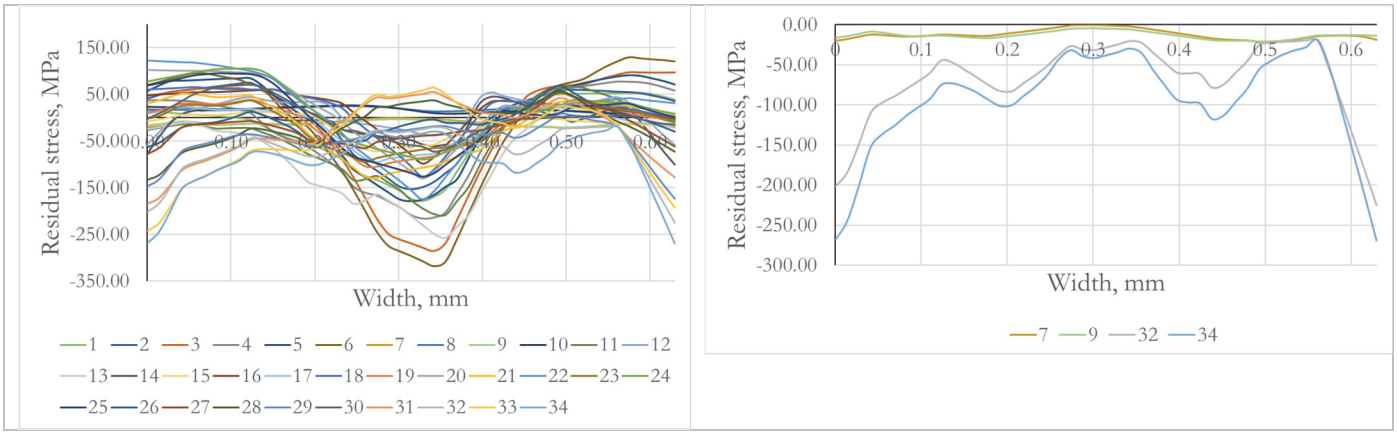

Figure 6: Residual stress for all calculated variants (a) and for the best variants (b).

Conclusions

The purpose of this work is a finite element study of residual stress distribution on thin blade edges after double-sided symmetric LSP at different machining parameters. The model used for calculation does not take into account the interaction of the laser beam with the treated surface, leading to the formation of plasma. The mechanical problem of elastic-plastic wave propagation in the material was solved using the velocity-sensitive Johnson-Cook constitutive relation. The pressure pulse parameters were measured experimentally using PDV analysis.

To investigate the influence of machining parameters on residual stresses were performed 34 numerical calculations. The investigated area was peened by square and circular spots simultaneously from both sides. Square spots with side size of 1 mm and round spots with diameter of 2 mm were considered. During numerical modelling the impact power density, overlapping percentage and number of passes were varied. Residual stress profiles over the entire thickness of the machined blade edge were analysed. In future work it is planned to use the results of numerical modelling of the treated layer characteristics at different parameters of the LSP process to train and verify the operation of the artificial neural network.

The following main conclusions can be drawn on the basis of the obtained results.

• Numerical modeling helps to estimate residual stress distribution after different processing modes during double-sided symmetric LSP, that allows to select the most appropriate machining modes for products with complex geometry.

• Low power density (3.18 GW/cm^2) cannot induce compressive residual stress after double-sided symmetric LSP on the treated surface.

• Circle spot with 30% overlapping, two passes and 21.98 or 25.48 GW/cm^2 power density allows to obtain compressive residual stresses over the entire thickness of the treated area. Moreover, the surface of residual stress distribution becomes more homogeneous. Other combinations of machining parameters lead to tensile residual stresses either on the treated surface or along the thickness of the treated area.

Acknowledgments

This study was carried out under the Agreement for the provision of grant funding from the federal budget for large scientific projects in priority areas of scientific and technological development of the Russian Ministry of Science and Higher Education no. 075-15-2024-552

References

[1] Liu, Y. H., Gu, X., Deng, D. X., et al. (2023). Research progress of double-sided laser shock peening technology[J]. Opto-Electron Eng. 50(4): 220186. DOI: 10.12086/oee.2023.220186.

[2] Wang, M., Chen, X., Dai, F., Siddiquee, A., Konovalov, S. (2024). Effects of different laser shock processes on the surface morphology and roughness of TC4 titanium alloy. Journal of Materials Processing Technology. 325. 118301. DOI: 10.1016/j.jmatprotec.2024.118301.
[3] Zhang, X., Li, H., Duan, S., Yu, X., Feng, J., Wang, B., Huang, Z. (2015). Modeling of residual stress field induced in Ti–6Al–4V alloy plate by two sided laser shock processing. Surface and Coatings Technology. 280. pp. 163-173. DOI: 10.1016/j.surfcoat.2015.09.004.
[4] Cai, M., Li, H., Shen, S., Lu, J., Zheng, B. (2024). Laser shock peening induced mechanical properties enhancement of 50CrVA alloy. Optics & Laser Technology. 169. 110180. DOI: 10.1016/j.optlastec.2023.110180.
[5] Umapathi, A., Swaroop, S. (2019). Mechanical properties of a laser peened Ti-6Al-4V. Optics & Laser Technology. 119. 105568. DOI: 10.1016/j.optlastec.2019.105568.
[6] Ebrahimi, M., Amini, S. and Mahdavi, S. M. (2017). The investigation of laser shock peening effects on corrosion and hardness properties of ANSI 316L stainless steel. The International Journal of Advanced Manufacturing Technology. 88. pp. 1557-1565. DOI: 10.1007/s00170-016-8873-0.
[7] Kong, M., Zang, T., Wang, Z., Zhu, L., Zheng, H., Gao, S., Ngwangwa, H.M. (2023). A study on the tribological behavior of AZ31 magnesium alloy sheets processed by temperature-assisted ultrasonic shot peening. Journal of Materials Research and Technology. 27. pp. 1223-1241. DOI: 10.1016/j.jmrt.2023.09.293.
[8] Zhu, Q., Lan, H., Lin, B., Wang, D., Huang, S., et al. (2023). Study on microstructure evolution. mechanical properties and deformation mechanism of Ti-6Al-4V alloy by hydraulic tension on-line warm rolling. Journal of Alloys and Compounds. 968. 171964. DOI: 10.1016/j.jallcom.2023.171964.
[9] Braisted, W., Brockman, R. (1999). Finite element simulation of laser shock peening. International Journal of Fatigue. 21. 7. pp. 719-724. DOI: 10.1016/S0142-1123(99)00035-3.
[10] King, A., Steuwer, A., Woodward, C., Withers, P.J. (2006). Effects of fatigue and fretting on residual stresses introduced by laser shock peening. Materials Science and Engineering: A. 435–436. pp. 12-18. DOI: 10.1016/j.msea.2006.07.020.
[11] Liao, Y., Ye, C., Cheng, G. J. (2016). [INVITED] A review: Warm laser shock peening and related laser processing technique. Optics & Laser Technology. 78. pp. 15–24. DOI:10.1016/j.optlastec.2015.
[12] Ruschau, J.J., John, R., Thompson. S.R., Nicholas, T. (1999). Fatigue crack nucleation and growth rate behavior of laser shock peened titanium. Int. J. Fatigue. 21. pp. 199-209. DOI: 10.1016/S0142-1123(99)00072-9.
[13] Kostina, A., Zhelnin, M., Gachegova, E., Prokhorov, A., Vshivkov, A., Plekhov, O. and Swaroop, S. (2022). Finite-element study of residual stress distribution in Ti-6Al-4V alloy treated by laser shock peening with varying parameters. Frattura ed Integrità Strutturale. 16(61). pp. 419–436. DOI: 10.3221/IGF-ESIS.61.28.
[14] Tang, Y., Li, S., Liao, Y., Ma, Y., Wu, X., Chi, Y., Lin, C., Zhang, Y. (2024). Improvement of fatigue life of Ti-6Al-4V alloy treated by double-sided symmetric oblique laser shock peening. Materials Today Communications. 39. 109121. DOI: 10.1016/j.mtcomm.2024.109121.
[15] Keller, S., Chupakhin., S., Staron, P., Maawad, E., Kashaev, N. and Klusemann, B. (2018). Experimental and numerical investigation of residual stresses in laser shock peened AA2198. J. Mater. Process. Technol.. 255. pp. 294-307. DOI: 10.1016/j.jmatprotec.2017.11.023.
[16] Rendler, N.J., Vigness, I. (1966). Hole-drilling strain-gage method of measuring residual stresses. Experimental Mechanics. 6. pp. 577–586. DOI: 10.1007/BF02326825.
[17] Ren, X., Chen, B., Jiao, J., Yang, Y., Zhou, W., and Tong, Z. (2020). Fatigue behavior of double-sided laser shock peened Ti-6Al-4V thin blade subjected to foreign object damage. Optics & Laser Technology. 121. 105784. DOI: 10.1016/j.optlastec.2019.